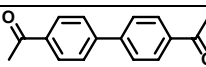
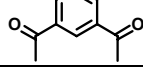
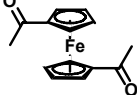


Supplementary Information

A new route to porous monolithic organic frameworks *via* cyclotrimerization

By Marcus Rose, Nicole Klein, Irena Senkovska, Christian Schrage, Philipp Wollmann, Winfried Böhlmann, Bertram Böhringer, Sven Fichtner, and Stefan Kaskel*

Table S1: Porosity of OFC-2 to OFC-4

Linker	OFC-	Specific surface area (BET, $p/p_0=0.3$) / m^2g^{-1}	
		A	B
	2	650	12 (565 ^a)
	3	8	273
	4	40	399

^aSynthesis in a solution (toluene) instead of a solvent-free melt.

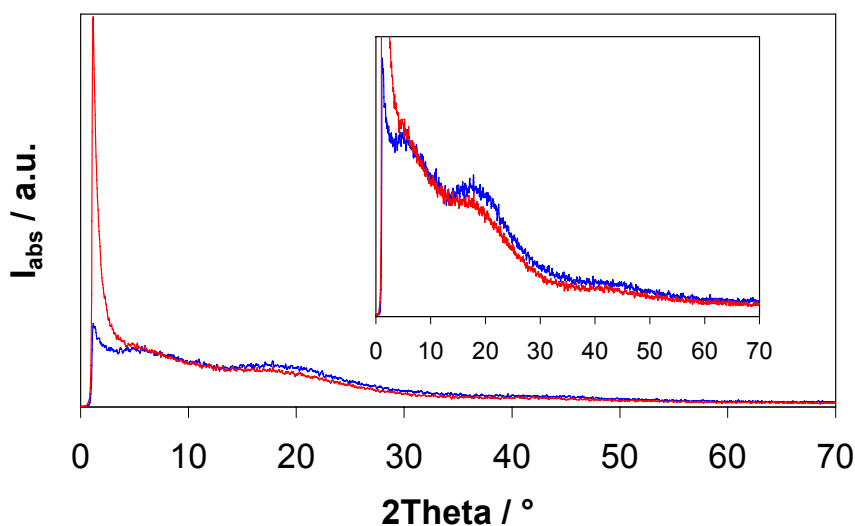


Figure S1. Powder XRD patterns for OFC-1A (blue) and OFC-1B (red) confirming an amorphous structure for the products of both synthetic routes.



Figure S2. Photographs of the OFC-1A synthesis in solution (0.2 g 14DAB in 60 ml Ethanol/Toluene (5:1)), taken directly after the addition of different amounts of SiCl_4 (from the left to the right image: 0 ml, 8 ml, 10 ml, 12 ml, 12 ml after 30 min).

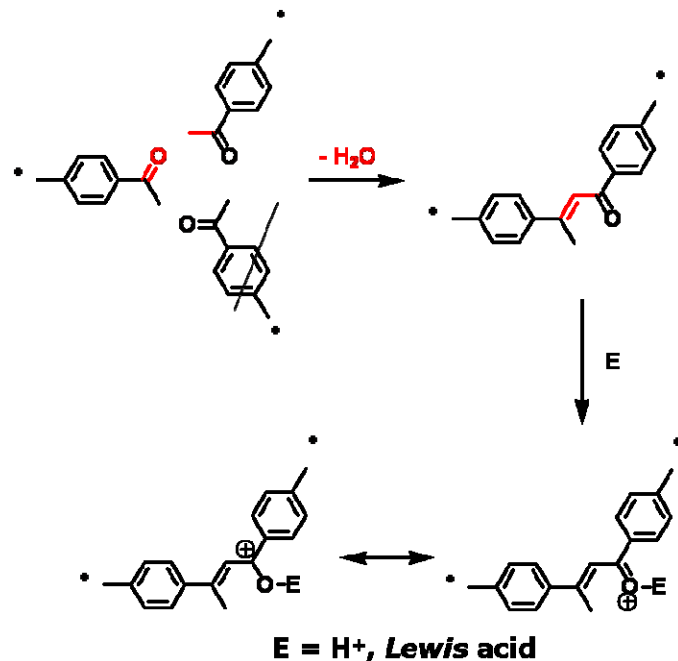


Figure S3. Dimerization reaction of two acetyl groups as a conceivable side reaction to the cyclotrimerization. Reaction with an electrophil E (e.g. *Lewis acid* or proton) can lead to a partial oxidation of the π -electron system and the resulting black color.

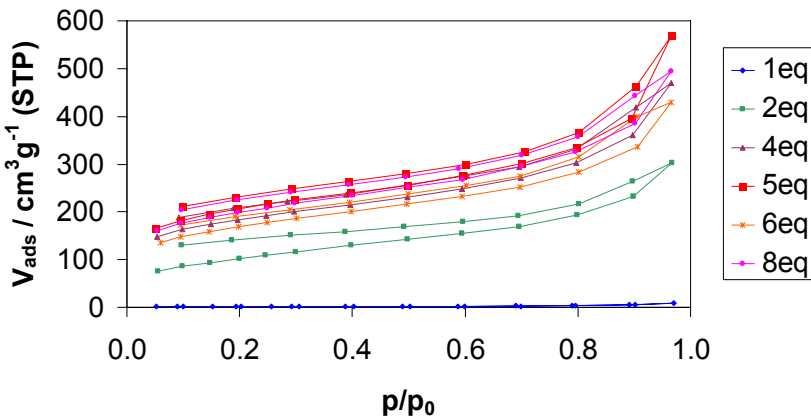


Figure S4. Porosity of OFC-1A in dependence of the amount of 4-toluene sulfonic acid relative to the educt amount.

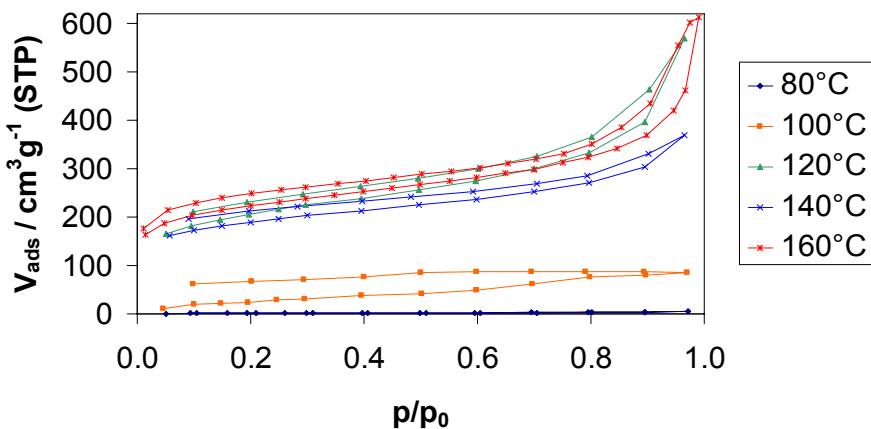


Figure S5. Porosity of OFC-1A in dependence of the reaction temperature.

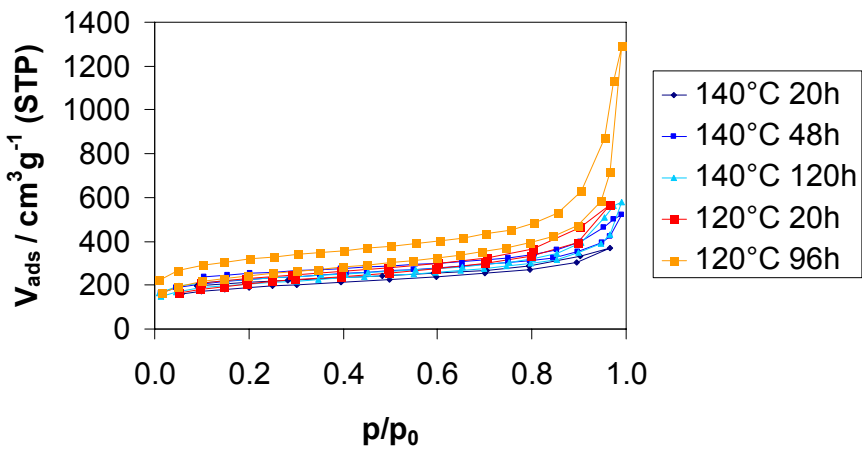


Fig. S6. Porosity of OFC-1A in dependence of the amount of the reaction time.

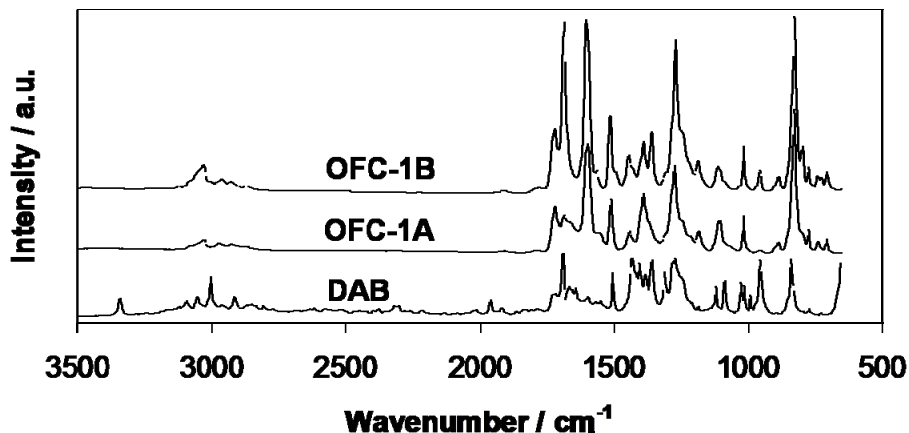


Figure S7. FTIR spectra of 1,4-diacetylbenzene (bottom), OFC-1A (middle) and OFC-1B (top) measured in diffuse reflexion mode.

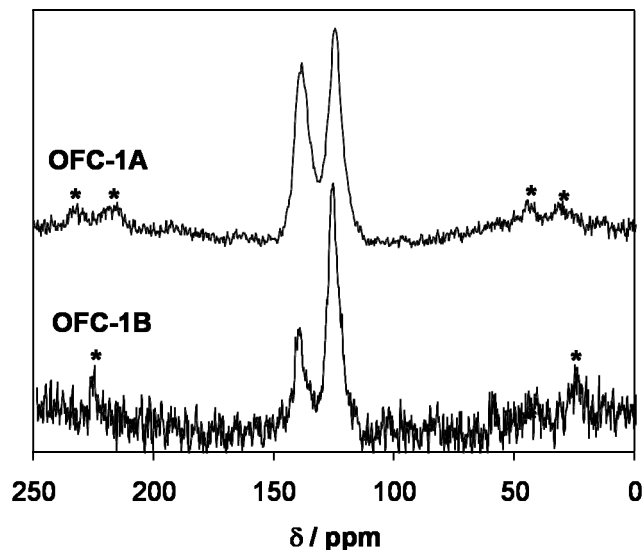


Figure S8. ¹³C CP MAS NMR spectra of OFC-1A and -1B revealing aromatic carbon atoms.

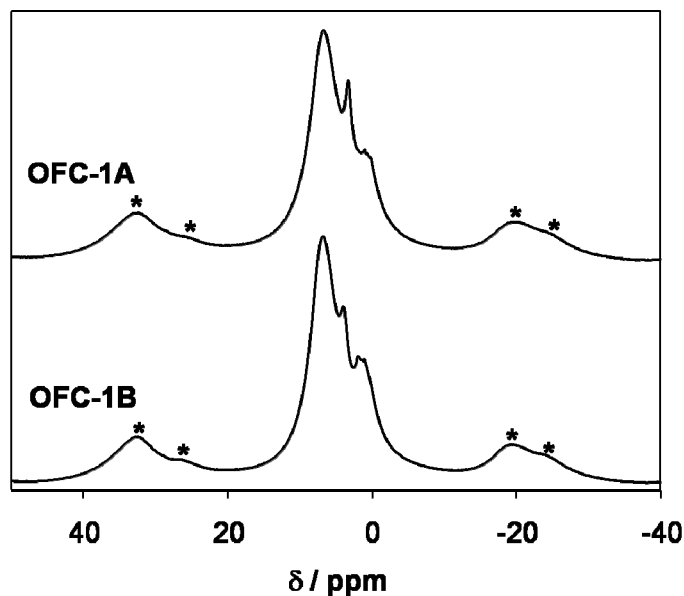


Figure S9. ¹H MAS NMR spectra of OFC-1A and -1B reveal aromatic and aliphatic C-H groups indicating an incomplete cross-linking.

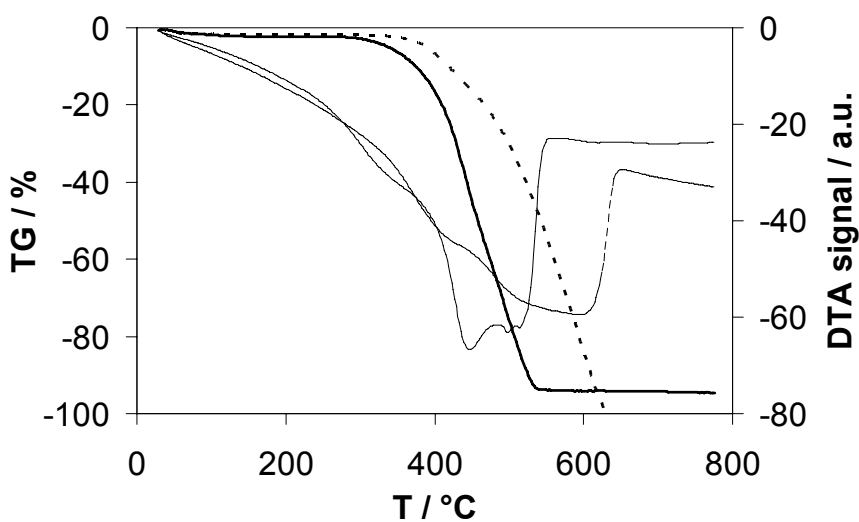


Figure S10. DTA (small lines) and TG (bold lines) of OFC-1A (filled lines) and OFC-1B (dashed lines).

Table S2. Results of the EDX analysis (wt-%).

OFC-1A		OFC-1B	
C	97.35	C	98.43
O	1.34	O	1.57
N	1.17	S	0
Na	0.13		

Table S3. Results of the elemental analysis and comparison with theoretical values (wt-%).

^aEstimated as the non C,H atoms (residue).

Experimental	OFC		Theoretical composition		
	1A	1B	100% CT	100% Dim	0% Reaction
			= C_{10}H_6	= 50% CT = $\text{C}_{10}\text{H}_8\text{O}$	(14DAB) = $\text{C}_{10}\text{H}_{10}\text{O}_2$
C	82.9	87.0	C	95.2	83.3
H	4.9	4.9	H	4.8	5.6
O ^a	n.d.	8.1	O	-	11.1
H/C ratio in %	5.9	5.6		5.0	6.7
O ^a /C ratio in %	n.d.	9.3		0.0	13.3
N		1.0			
Na		0.1			

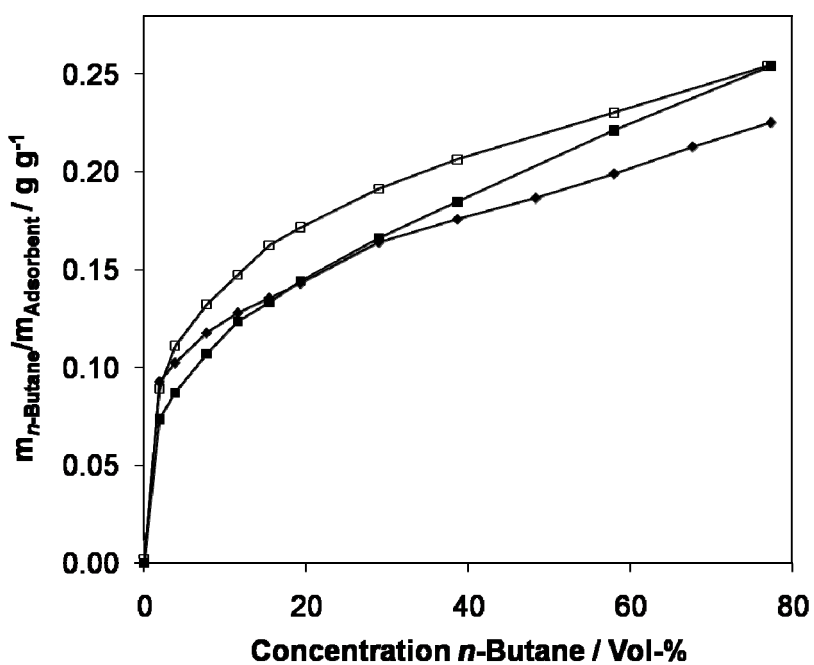


Figure S11. *n*-Butane physisorption isotherms of OFC-1A (diamonds) and OFC-1B (squares) measured at 30 °C. Filled symbols denote adsorption and empty symbols denote desorption, respectively.

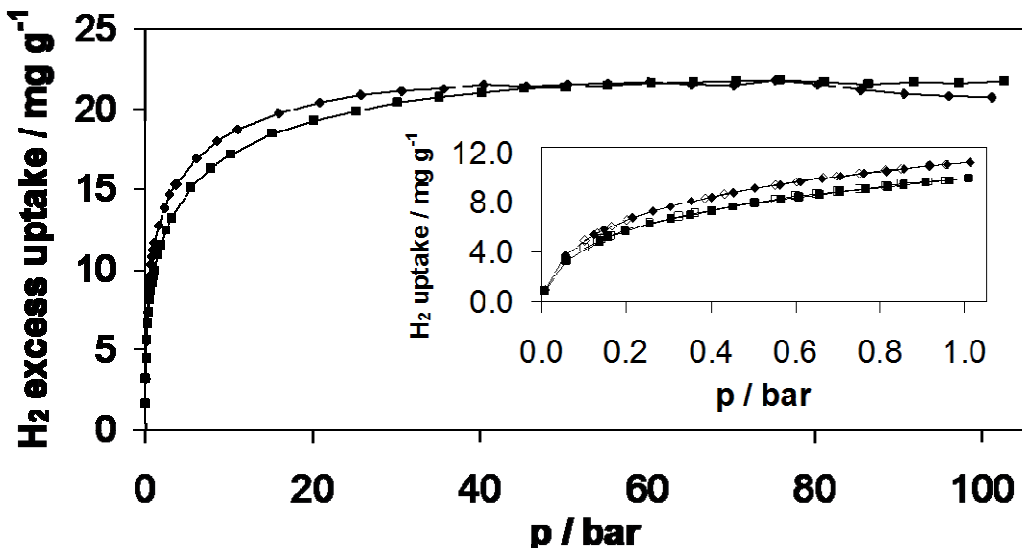


Figure S12. High pressure hydrogen adsorption of OFC-1A (diamonds) and OFC-1B (squares) measured at -196 °C. The inset shows the low pressure hydrogen physisorption isotherm measured up to 1 bar.

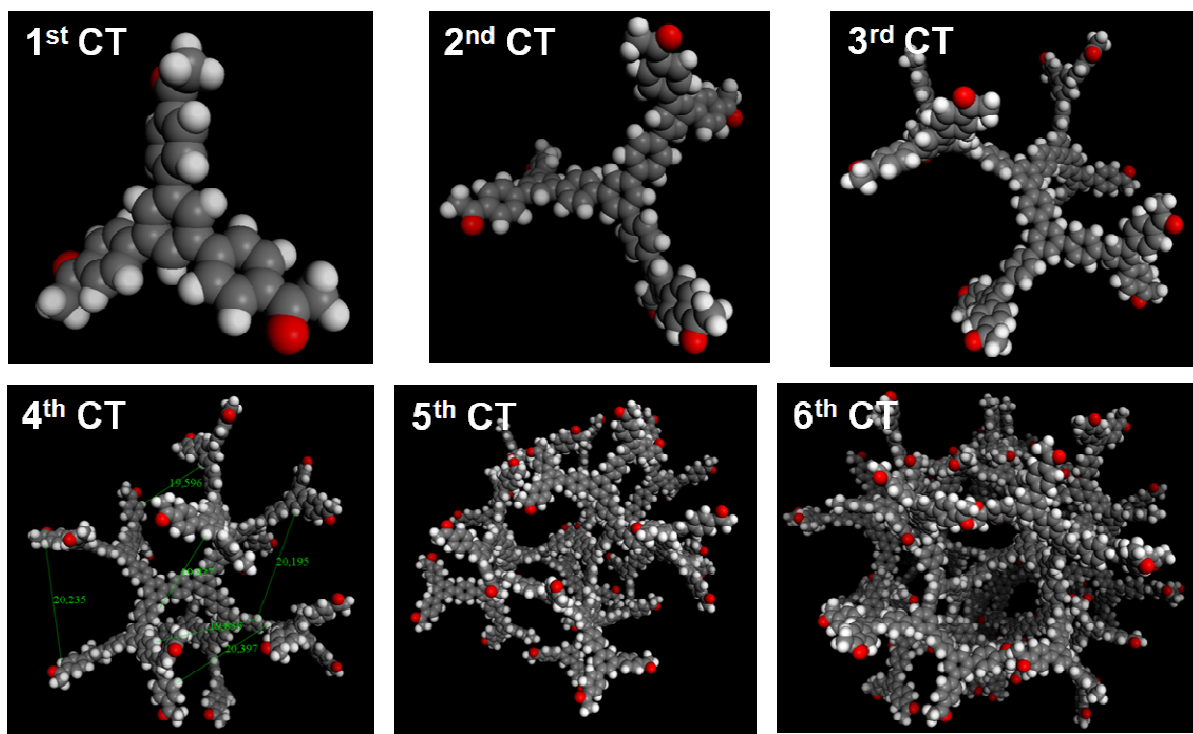


Figure S13. Strucutral simulations of a dendrimer of OFC-1 after different cyclotrimerization steps. Beginning with the 6th reaction step not all acetyl end groups are accessible for further reaction.